JMEPEG (1995) 4:441-448

Nitrided and Carbided Magnets

G.C. Hadjipanayis, Y.H. Zheng, A.S. Murthy, W. Gong, and F.M. Yang

In this article, we review our recent studies on new rare-earth intermetallic compounds including the Ga, Si substituted 2:17-type compounds, their nitrides, carbides, and the $Sm_3(Fe,Ti)_{29}N_5$ compounds. Much of our recent work is focused on the $Sm_2(Fe,Ga)_{17}C_x$ alloys where we used melt spinning and subsequent annealing to obtain high coercivity. The highest coercivity obtained so far was in $Sm_2Fe_{14}Ga_3C_{2.5}$ with a value of 12.8 kOe at room temperature. The off-stoichiometric $Sm_2Fe_{14-x}Co_xSi_2N_y$ nitrides maintain the Th_2Zn_{17}-type structure but with a unit-cell expansion $\Delta V/V$ up to 5% compared to the host materials. The $Sm_2Fe_{14-x}Co_xSi_2C_z$ carbides maintain the Th_2Zn_{17}-type structure when $z = 1$ and transform to the $BaCd_{11}$-type structure when $z = 2$. A very large anisotropy field with an applied magnetic field (H_a) value of 227 kOe for $Sm_2Fe_{14}Si_2N_{2.6}$ and 276 kOe for $Sm_2Fe_{10}Co_4Si_2N_{2.3}$ is observed at low temperature (1.5 K). The $Sm_3(Fe,Ti)_{29}N_5$ compound and its nitrides show very interesting magnetic properties. Both of these compounds exhibit ferromagnetic ordering with Curie temperature (T_c) of 486 and 750 K, respectively. The room temperature saturation magnetization is 119 emu/g for the parent compounds and 145 emu/g for the nitrides. The easy magnetization direction changes from planar to uniaxial upon nitrogenation. The anisotropy field for the nitrides is 12 T at room temperature and 25 T at 4.2 K.

Keywords

anisotropy field, annealing effect, coercivity, ferromagnetic ribbons, high field measurement

1. Introduction

FOR a long time, the R_2Fe_{17} intermetallic compounds were not considered as potential permanent magnet materials because of their low Curie temperature and planar magnetocrystalline anisotropy. However, after the discovery of the gas-phase interstitial modification (GIM) process, it was found that interstitial Sm_2Fe_{17} nitrides and carbides have dramatically improved magnetic properties over those of the parent compounds, making them suitable candidates for permanent magnets (Ref 1, 2). These materials are highly metastable; they decompose into RN(C) and αFe upon heating to 700 °C. The problem of decomposition was partially solved in arc-melted $R_2Fe_{17}C_x$, where Fe_3C was used to form the ternary carbides, but the carbon content is well below 2, with $x = 1.5$ for heavy rare-earth elements and $x = 1$ for light rare-earth elements (Ref 3, 4). Recently, it was discovered that substitution of Ga for Fe in $Sm_2Fe_{17}C_x$ helps the formation of high-carbon, rare-earth compounds with the 2:17-type structure (Ref 5, 6). We extensively studied the structural and magnetic properties of melt-spun alloys with compositions $Sm_2Fe_{17-x}M_xC_y$ (M = Ga, Al) (Ref 7) where optimization studies in composition and heat treatment were made to obtain a high value of coercivity.

The incorporation of Si atoms in the lattice of R_2Fe_{17} significantly enhanced the Curie temperature and produced spin-reorientation transition region in the Er_2Fe_{17} alloy system (Ref 8, 9). The off-stoichiometric compounds $R_2Fe_{14-x}Co_xSi_2$ with R = Y or a heavy rare-earth element were studied and found to have interesting properties (Ref 10). Substitution of Co for Fe led to an increase in the Curie temperature and spin reorientation temperature in several compounds. However, due to the antiferromagnetic coupling between the heavy rare-earth and transition metal atom moments, the saturation magnetization of these compounds is very low, and none of them exhibit a uniaxial anisotropy at room temperature. We recently extended these studies to the compounds with R = Sm, its nitrides and carbides.

Very recently, a novel ternary $Nd_2(Fe,Ti)_{19}$ intermetallic phase was reported (Ref 11). The composition of this phase is $Nd_3(Fe,Ti)_{29}$, and its structure is an intermediate phase between the 1:12 and 2:17 type structure. The new phase was also obtained with R = Sm (Ref 12). The $Sm_3(Fe,Ti)_{29}$ compound exhibited a ferromagnetic coupling with a Curie temperature around 486 K, but with a planar anisotropy. We recently prepared the $Sm_3(Fe,Ti)_{29}$ nitrides and investigated their structural and magnetic properties with emphasis on the magnetocrystalline anisotropy.

2. Experimental

Samples with desired composition were prepared by arc melting the constituent materials with at least 99.9% purity under purified argon gas. An excess of 5 to 15% Sm was added to compensate for the Sm loss during arc melting because of its high vapor pressure. After arc melting, the alloys were vacuum annealed at 1000 to 1100 °C for 1 to 24 h to get a single phase. The carbides were obtained by arc melting using the Fe_3C alloy as the carbon-containing material. The nitrides were obtained by the GIM method. The ingots were pulverized to an average particle size of about 20 to 30 μm, and the powder samples obtained were then heated in purified N_2 gas under a pressure of about 1.7 atm at 770 to 870 K for 10 to 60 h to form the nitrides. The crystal structure studies were made by x-ray diffraction (XRD) using a Cu-Kα radiation. XRD patterns on aligned powder samples were used to determine the easy magnetization direction of the compounds. Thermomagnetic curves were measured using a vibrating sample magnetometer (VSM) with an applied field of 500 Oe. The magnetization curves were measured using a superconducting quantum interference de-

G.C. Hadjipanayis, Y.H. Zheng, A.S. Murthy, and W. Gong, Dept. of Physics and Astronomy, University of Delaware, DE 19716, USA; and **F.M. Yang,** Institute of Physics, Chinese Academy of Science, Beijing, China.

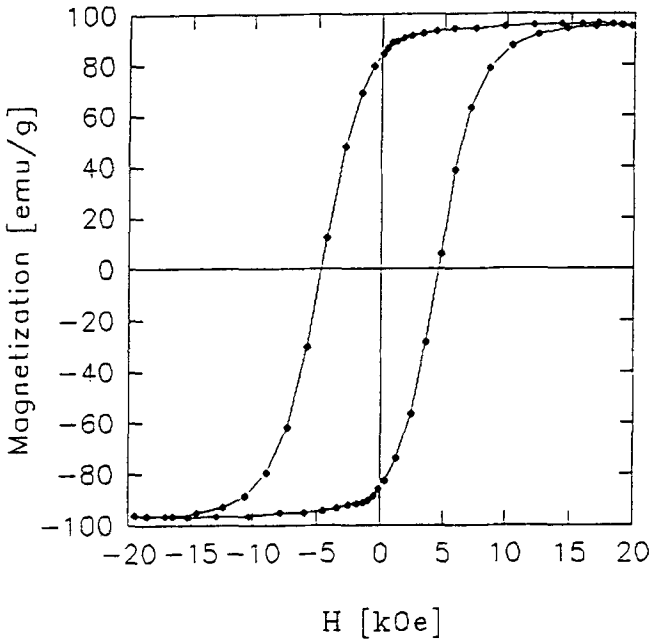

Fig. 1 Hysteresis loop of an aligned $Sm_2Fe_{14}Ga_3C_{2.5}$ powder sample measured in the alignment direction

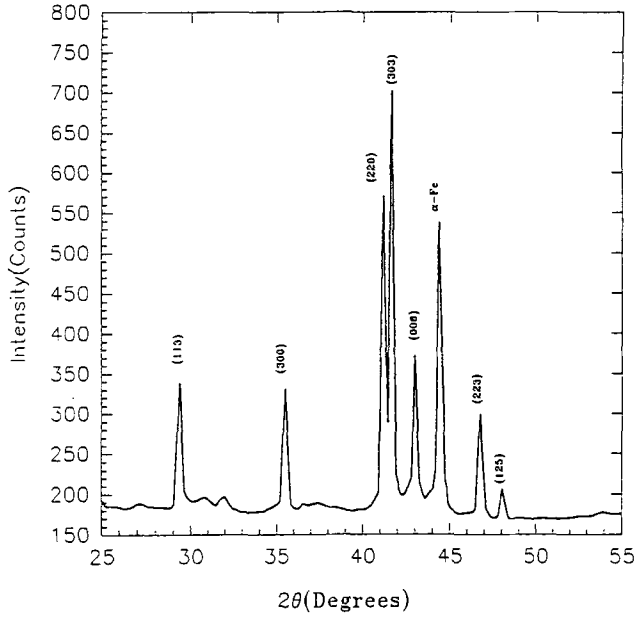

Fig. 2 XRD pattern of $Sm_2Fe_{15}Ga_2C_2$ annealed at 800 °C for 20 min

vice (SQUID) magnetometer with an applied field of 55 kOe and at temperatures between 4.2 K and room temperature. The anisotropy field was determined from magnetization curves measured along and perpendicular to the alignment direction. The high field magnetization curves were measured with an applied field of 35 T at 4.2 K in the high field installation at the University of Amsterdam.

3. Results and Discussion

3.1 $Sm_2Fe_{17-x}Ga_xC_y$

XRD measurements showed that the as-cast $Sm_2Fe_{14}Ga_3C_x$ compounds ($x = 1$, 1.5, 2, 2.5) have a single phase with the Th_2Zn_{17}-type structure. An attempt was first made to prepare powders from the as-cast samples. Figure 1 shows the hysteresis loop of a powder sample with a composition $Sm_2Fe_{14}Ga_3C_{2.5}$ aligned in molten wax using an applied field of 20 kOe and then measured in a direction parallel to the alignment direction. The data showed a substantial coercivity of 4.5 kOe and a saturation magnetization, M_{sat}, of 88 emu/g. The high coercivity suggests a high anisotropy field for the $Sm_2(Fe,Ga)_{17}C_x$ phase.

The as-spun ribbons obtained for all compositions were amorphous. The ribbons were subsequently annealed to be crystallized into the 2:17-type phase (Fig. 2). The effect of annealing temperature on coercive force (H_c) is shown in Fig. 3 for the $Sm_2Fe_{15}Ga_2C_2$ samples. At each annealing temperature, the samples were annealed for 20 min. H_c reached a maximum value of 12 kOe for $Sm_2Fe_{15}Ga_2C_2$ samples when annealed at a temperature of 850 °C. Similar results were also observed for the $Sm_2Fe_{14}Ga_3C_{2.5}$ samples (Fig. 3). A maximum value of H_c of around 12.8 kOe was observed in samples with composition $Sm_2Fe_{14}Ga_3C_{2.5}$ after annealing at 800 °C for 20 min.

The demagnetization curves of the samples that were annealed at a higher temperature of 800 °C indicated the presence of two phases with coarse grains (Fig. 4), which were found to be αFe and the 2:17-type phases (Fig. 2). Annealing at a lower temperature of about 700 °C was also conducted, and the coercivity obtained was significantly lower ($H_c \approx 5$ kOe), but the reduced remanence, m_R, was much higher (68%) than that obtained at higher annealing temperatures. In this annealing condition, the coercivity did not change appreciably with annealing time, for times in the range of 20 to 90 min.

The transmission electron microscopy (TEM) studies carried out for ribbon samples of $Sm_2Fe_{15-x}Ga_xC_y$ ($x = 2$, 3 and $y = 1$, 1.5, 2, 2.5) annealed at temperatures ranging from 700 to 850 °C all indicated the presence of a mixture of αFe and 2:17-type phases. Figure 5 shows a typical dark-field image with the corresponding diffraction pattern for a ribbon sample of $Sm_2Fe_{15}Ga_2C_2$ annealed at 700 °C for 20 min. From this dark-field image, besides grains that measured approximately 25 nm, very fine features with an appearance of a mottled structure are present on a nano-scale. These features measuring a few nanometers could be characterized as due to a very fine-grained 2:17 phase present along with a αFe phase. This observation of such a fine-grained structure agrees well with the XRD results where the peaks corresponding to both 2:17-type and αFephases were highly broadened. These samples also gave rise to a smooth demagnetization curve with a high reduced remanence, a behavior characteristic of "exchange-coupled" magnets consisting of a mixture of fine-grained hard and soft phases. The TEM studies carried out for samples of the same composition, but annealed at 800 °C, indicated a substantial increase in the grain size. Figure 6 shows a typical dark-field im-

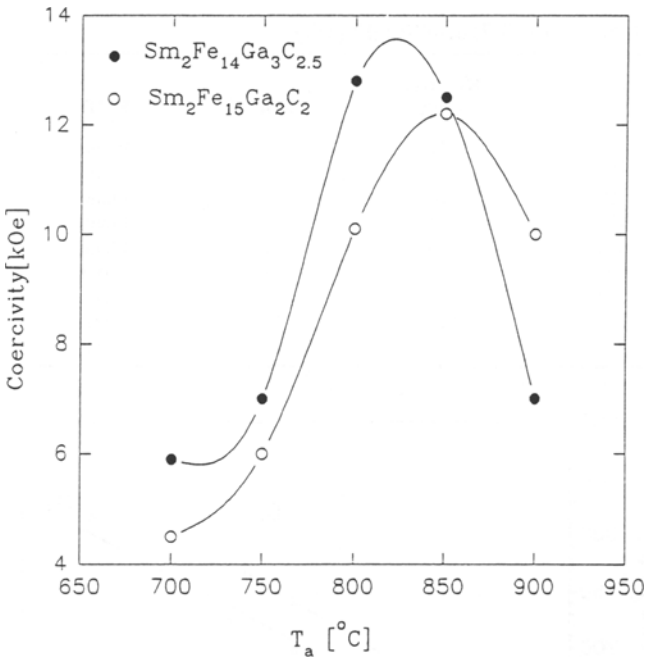

Fig. 3 Dependence of coercivity on annealing temperature (annealing time = 20 min) for $Sm_2Fe_{15}Ga_2C_2$ and $Sm_2Fe_{14}Ga_3C_{2.5}$

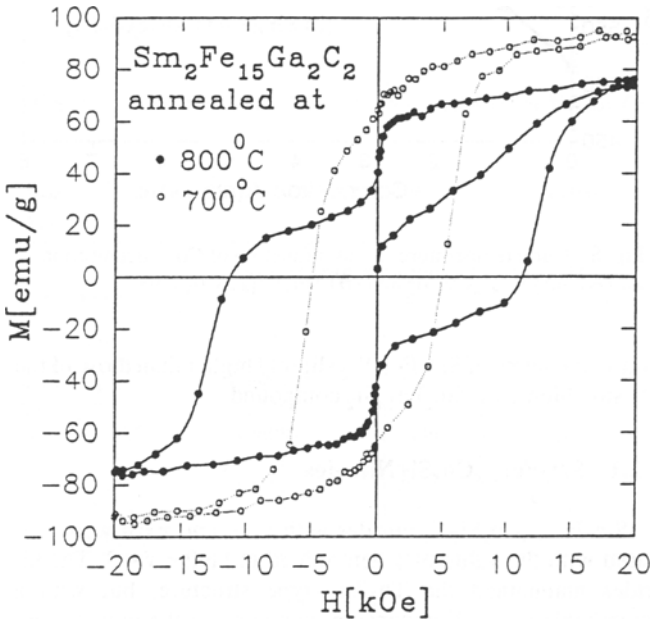

Fig. 4 Hysteresis loops of $Sm_2Fe_{15}Ga_2C_2$ ribbons annealed at 800 and 700 °C for 20 min. The demagnetization curve is smoother when the ribbon was annealed at 700 °C.

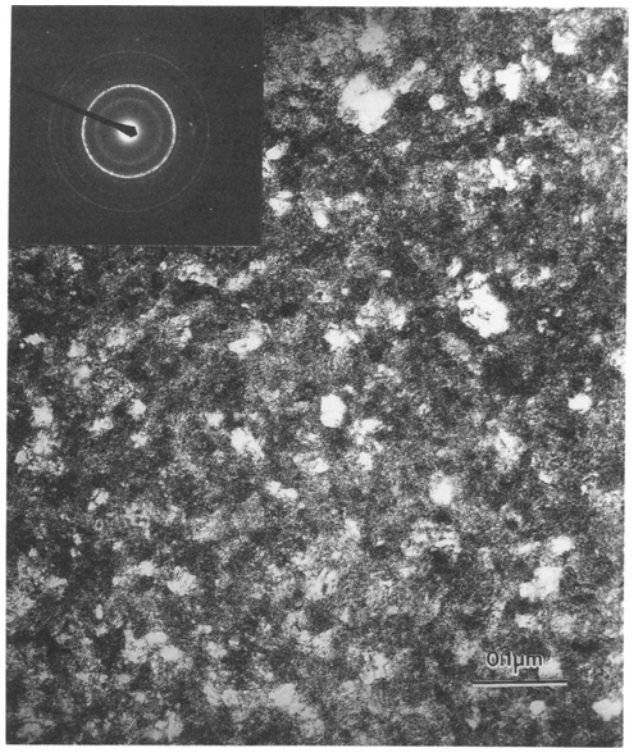

Fig. 5 Dark-field image of an $Sm_2Fe_{15}Ga_2C_2$ ribbon sample annealed at 700 °C for 20 min. The selected-area diffraction pattern shown in the inset corresponds to a mixture of αFe and 2:17-type phase.

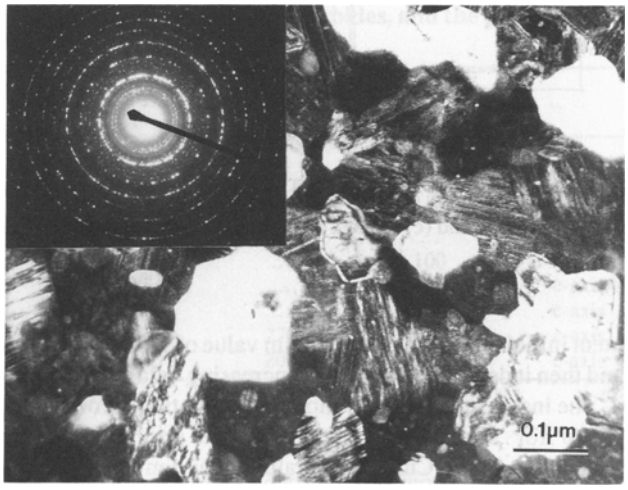

Fig. 6 Dark-field image with a diffraction pattern of a $Sm_2Fe_{15}Ga_2C_2$ ribbon sample annealed at 800 °C for 20 min

age for a sample of $Sm_2Fe_{15}Ga_2C_2$ annealed at 800 °C for 20 min. The average grain size in these samples is about 100 nm.

3.2 $Sm_2Fe_{14-x}Co_xSi_2$ Compounds

XRD and thermomagnetic analysis (TMA) data showed that all the investigated $Sm_2Fe_{14-x}Co_xSi_2$ compounds had a single Th_2Zn_{17}-type phase (Fig. 7). Substitution of Co for Fe did not lead to any change in the crystal structure even for $x = 14$. Figure 8 shows the Curie temperature, T_c, as a function of Co concentration. T_c increases almost linearly with Co content, from 514 K for $x = 0$ to 817 K for $x = 7$ with an average increase of 55 K per Co atom. The saturation magnetization at room temperature as a function of Co content is shown in Table 1. The saturation magnetization, M_{sat}, increases with increasing Co

Table 1 Lattice parameters, V, T_c, M_{sat}, H_a, and EMD in $Sm_2Fe_{14-x}Co_xSi_2$ (x = 0-7) and $Sm_2Fe_{15}Si_2$

Compound	Lattice parameters, nm a	c	Volume, nm^3	T_c, K	M_{sat}, H_a, emu/g	kOe	EMD
$Sm_2Fe_{15}Si_2$	0.8502	1.2414	777.711	512	127	...	Plane
$Sm_2Fe_{14}Si_2$	0.8484	1.2340	77.278	514	118	...	Plane
$Sm_2Fe_{13}CoSi_2$	0.8477	1.2388	77.087	569	120	...	Plane
$Sm_2Fe_{12}Co_2Si_2$	0.8478	1.2613	77.433	624	123	...	Plane
$Sm_2Fe_{11}Co_3Si_2$	0.8456	1.2338	76.400	672	124	...	Plane
$Sm_2Fe_{10}Co_4Si_2$	0.8459	1.2379	76.462	698	124	8	c-axis
$Sm_2Fe_9Co_5Si_2$	0.8439	1.2338	76.088	724	122	13	c-axis
$Sm_2Fe_8Co_6Si_2$	0.8414	1.2301	75.396	775	120	21	c-axis
$Sm_2Fe_7Co_7Si_2$	0.8404	1.2293	75.128	817	112	23	c-axis

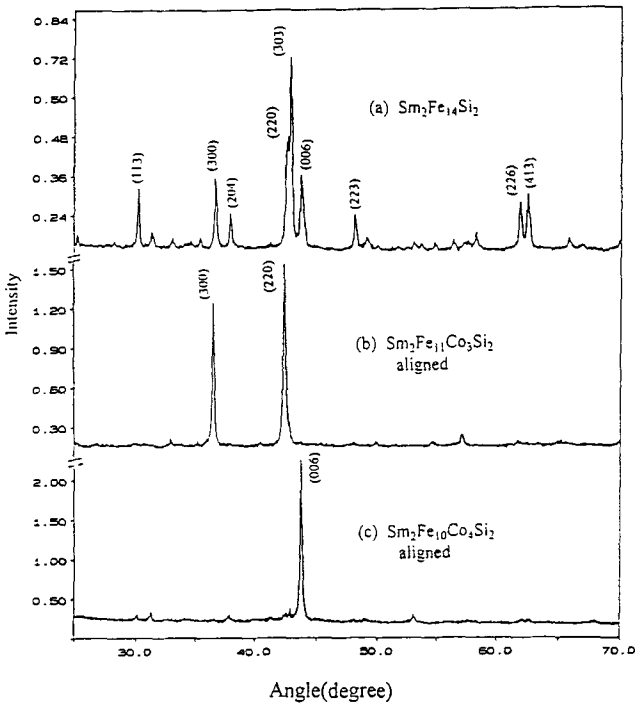

Fig. 7 XRD patterns of (a) $Sm_2Fe_{14}Si_2$, (b) aligned $Sm_2Fe_{11}Co_3Si_2$, and (c) aligned $Sm_2Fe_{14-x}Co_xSi_2$ samples

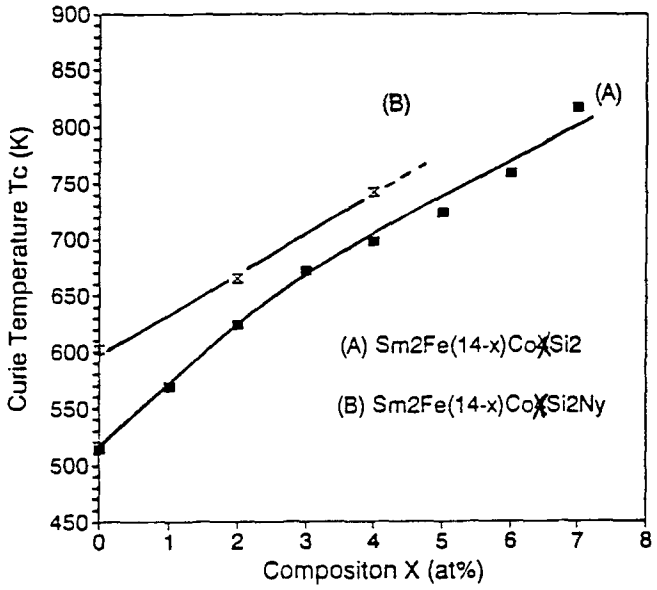

Fig. 8 Curie temperature, T_c, as a function of Co concentration for (A) $Sm_2Fe_{14-x}Co_xSi_2$ and (B) $Sm_2Fe_{14-x}Co_xSi_2N_y$

content initially reaching a maximum value of 124 emu/g at x = 3, and then it decreases for further increasing values of Co content. The increase of the saturation magnetization at room temperature for small Co content may be attributed to the enhancement in the Curie temperature. The $Sm_2Fe_{14-x}Co_xSi_2$ compounds exhibited a planar anisotropy when $x = 0$. The magnetocrystalline anisotropy changed from planar to uniaxial when $x \geq 4$. Figure 7 shows the XRD for the $x = 3$ and $x = 4$ aligned powder samples. For compounds with $x \leq 3$, a drastic increase in the (h k 0) reflections and disappearance of (0 0 1) reflection are observed, indicating that these samples have an easy planar anisotropy, in contrast with the compounds with $x \geq 4$. In the latter, only the (0 0 1) reflections are drastically increased implying a uniaxial anisotropy at room temperature.

For comparison, the properties of the stoichiometric $Sm_2Fe_{15}Si_2$ compound are also listed in Table 1. Both of them have a planar anisotropy with the saturation magnetization and unit-cell volume of $Sm_2Fe_{15}Si_2$ slightly higher than those of the off-stoichiometric $Sm_2Fe_{14}Si_2$ compound.

3.2.1 $Sm_2Fe_{14-x}Co_xSi_2$ Nitrides

$Sm_2Fe_{14-x}Co_xSi_2Y_y$ nitrides with $x = 0$ and $x = 4$ were prepared with the value of y determined to be $2 < y < 3$. The nitrides maintained the Th_2Zn_{17}-type structure, but with a remarkable unit-cell expansion compared to the parent compounds. The unit-cell volume expansion is 4.2% for $x = 0$ (y = 2.6) and 5% for $x = 4$ (y = 2.3). Introduction of nitrogen led to an increase in Curie temperature from 514 to 602 K for $x = 0$ and from 698 to 742 K for $x = 4$, respectively. The increase in T_c may be partially associated with the unit cell expansion. Introduction of nitrogen also changed the anisotropy in $Sm_2Fe_{14}Si_2$ from planar to uniaxial with a room temperature anisotropy field of H_a = 157 kOe. In $Sm_2Fe_{10}Co_4Si_2$ compounds, introduction of nitrogen led to an increase in the anisotropy from 8 kOe to 175 kOe. A very large anisotropy field was observed at low temperature (1.5 K) with the value of H_a = 227 kOe for $Sm_2Fe_{14}Si_2N_{2.6}$ and H_a = 276 kOe for $Sm_2Fe_{10}Co_4Si_2N_{2.3}$ (Table 2).

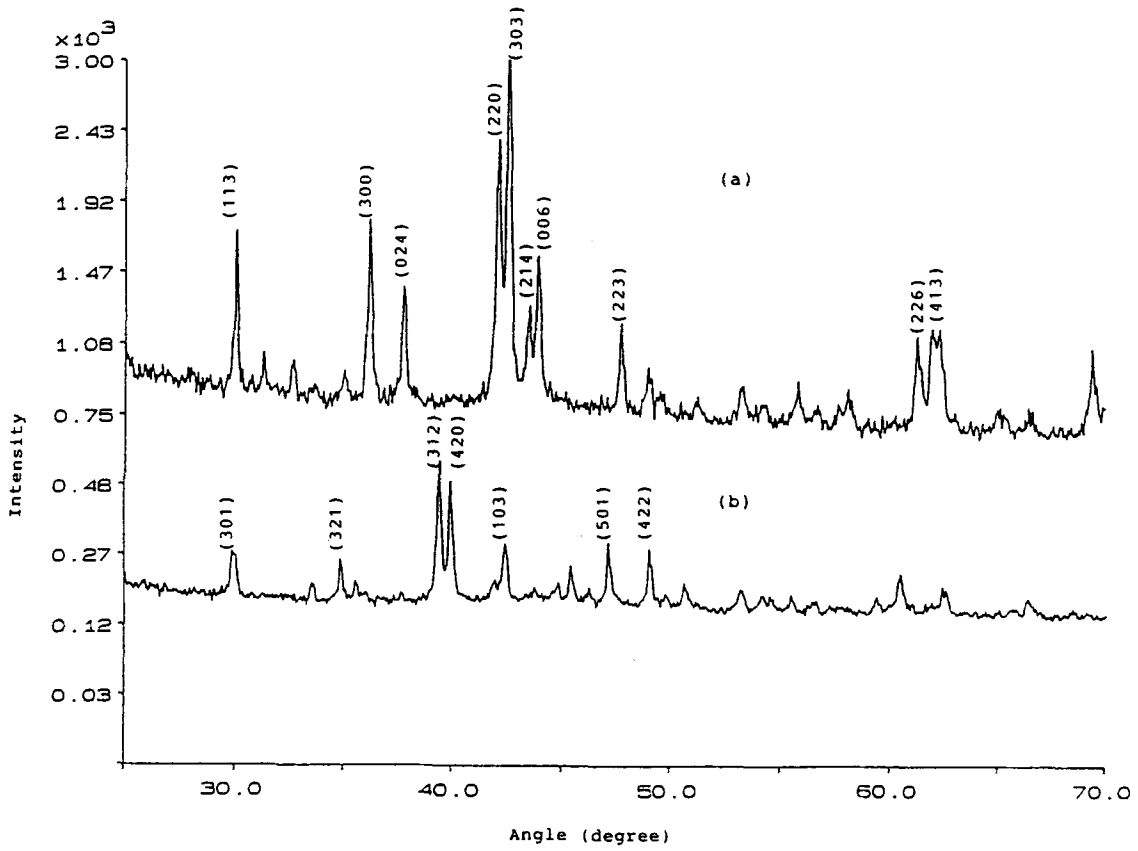

Fig. 9 XRD patterns of (a) $Sm_2Fe_{14}Si_2C$ and (b) $Sm_2Fe_{14}Si_2C_2$ samples

Table 2 Lattice parameters, unit-cell volume expansion, M_{sat}, T_c, H_a, and EMD for nitrides, carbides, and the parent compounds

Compounds	Lattice parameters, nm		$\Delta V/V$, M_{sat},	T_c, H_a, kOe				
	a	*c*	%	emu/g	K	1.5 K	300 K	
$Sm_2Fe_{14}Si_2$	0.8484	1.2340	...	118	514	...	...	Plane
$Sm_2Fe_{14}Si_2N_{2.6}$	0.8633	1.2478	4.2	117	602	227	157	c-axis
$Sm_2Fe_{14}Si_2C$	0.8591	1.2387	2.4	109	593	205	100	c-axis
$Sm_2Fe_{15}Si_2$	0.8502	1.2414	...	127	512	...	...	Plane
$Sm_2Fe_{15}Si_2C$	0.8608	1.2448	2.7	105	580	...	100	c-axis
$Sm_2Fe_{15}Si_2C_{1.5}$	0.8648	1.2478	4.0	101	590	...	110	c-axis
$Sm_2Fe_{10}Co_4Si_2$	0.8459	1.2379	...	124	698	...	8	c-axis
$Sm_2Fe_{10}Co_4Si_2N_{2.3}$	0.8633	1.246	5.0	113	742	276	175	c-axis
$Sm_2Fe_{10}Co_4Si_2C$	0.8525	1.238	1.5	111	731	204	80	c-axis

3.2.2 $Sm_2Fe_{14-x}Co_xSi_2$ Carbides

$Sm_2Fe_{14-x}Co_xSi_2C_z$ with $x = 0$ and $x = 4$ were prepared by arc melting. The values of z were chosen to be 0, 1, and 2. The carbides with $z = 1$ were of single 2:17-type phase structure, but those with $z = 2$ showed a major second phase structure as shown by XRD and thermomagnetic analysis (Fig. 9). This second phase is believed to be the $BaCd_{11}$-type. Previously, a phase transformation was reported in $RFe_{10}SiC_x$ alloys from the Th_2Zn_{17}-type structure to the $BaCd_{11}$-type structure, which was induced by gas-phase reaction (Ref 13). This phase transformation is seen again in the $Sm_2Fe_{14-x}Co_xSi_2C_z$ system. Note that the corresponding stoichiometric compound, $Sm_2Fe_{15}Si_2C_{1.5}$, showed a single Th_2Zn_{17}-type phase structure with an M_{sat} of 101 emu/g and a T_c of 590 K. The properties of stoichiometric $Sm_2Fe_{15}Si_2C_x$ compounds ($x = 1$, 1.5) are also included in Table 2.

Introduction of C led to an increase in lattice constants *a* and *c*, and an expansion in the unit-cell volume. However, the unit-cell expansion of carbides is smaller than that of the corresponding nitrides. Interstitial carbon atoms also led to an increase in the Curie temperature; the increase is about 80 K for $Sm_2Fe_{14}Si_2C$ and 30 K for $Sm_2Fe_{10}Co_4Si_2C$. Introduction of carbon also increased the contribution of the Sm sublattice to

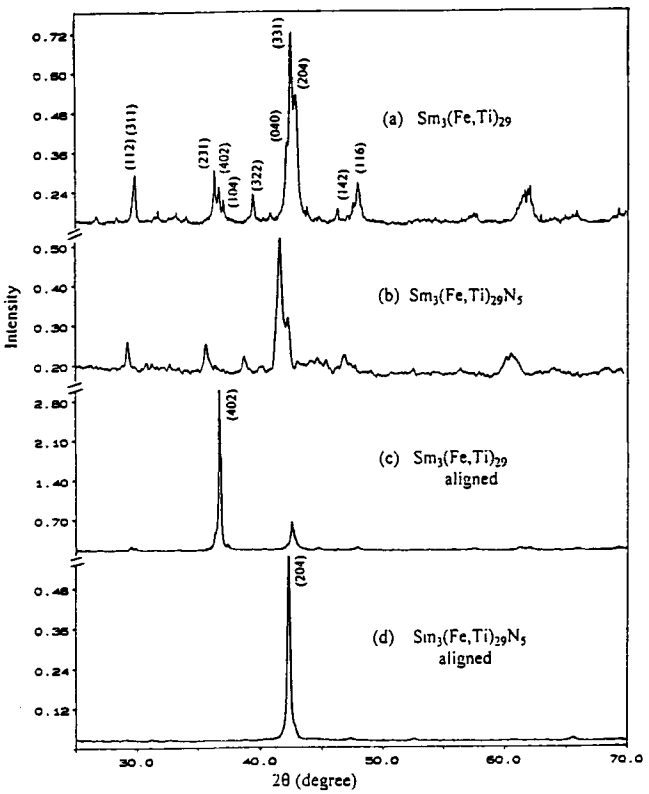

Fig. 10 XRD patterns of $Sm_3(Fe_{0.933}Ti_{0.067})_{29}$ and $Sm_3Fe_{0.0933}Ti_{0.067})_{29}N_5$ powders

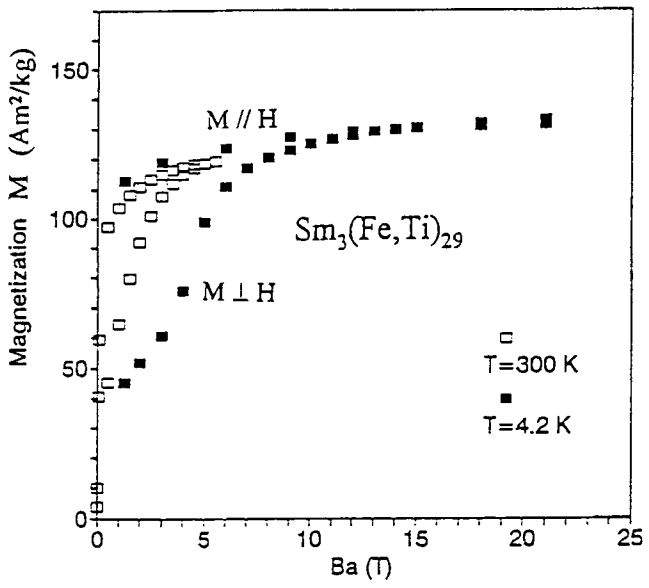

Fig. 11 Magnetization curves of aligned $Sm_3(Fe,Ti)_{29}$ powders measured parallel and perpendicular to the alignment direction

the uniaxial anisotropy and changed the anisotropy of $Sm_2Fe_{14}Si_2$ from planar to uniaxial. An H_a value of 100 kOe at 300 K and 205 kOe at 1.5 K was obtained for $Sm_2Fe_{14}Si_2C$. The anisotropy field of $Sm_2Fe_{10}Co_4Si_2C$ was H_a = 80 kOe at 300 K and 204 kOe at 1.5 K. Due to the smaller unit cell volume expansion, the increases in T_c and H_a were smaller than those of corresponding nitrides.

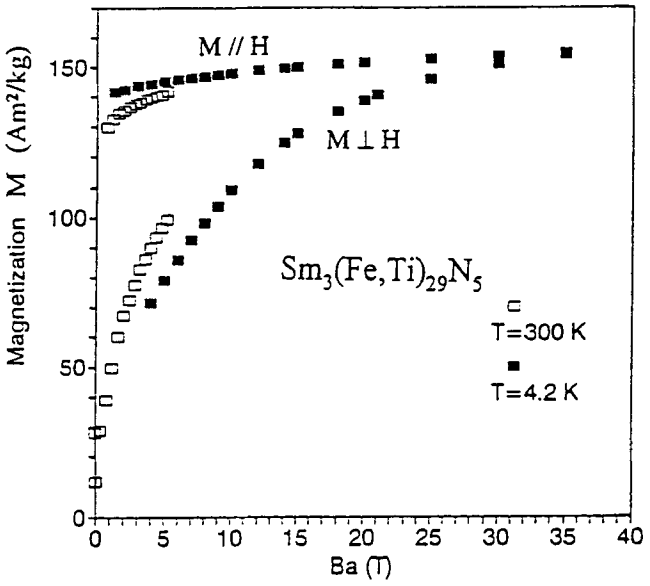

Fig. 12 Magnetization curves of aligned $Sm_3(Fe,Ti)_{29}N_5$ powders measured parallel and perpendicular to the alignment direction

3.3 $Sm_3(Fe_{0.933}Ti_{0.067})_{29}$

XRD and TMA show that the $Sm_3(Fe_{0.933}Ti_{0.067})_{29}$ compound is of single phase. The XRD patterns are shown in Fig. 10. All peaks were indexed on the basis of the $Nd_3(Fe,Ti)_{29}$-type structure. The lattice parameters are a = 1.065 nm, b = 0.858 nm, and c = 0.972 nm, and β = 96.98°.

The nitrides maintain the $Nd_3(Fe,Ti)_{29}$-type structure of the parent compound, but with the XRD peak shifted to the lower angles, suggesting an increase in the lattice parameter. The lattice parameters of the nitrides are a = 1.098 nm, b = 0.882 nm, and c = 0.985 nm, and β = 97.50°. The unit-cell volume expansion $\Delta V/V$ is 7% compared with the parent compounds. Nitrogen absorption also led to an increase in the Curie temperature. The T_c of the nitrides is 750 K, about 260 K higher than that of the host materials.

Magnetization measured along and perpendicular to the alignment direction at several temperatures is shown in Fig. 11 for the parent compounds and Fig. 12 for the nitrides. Introduction of nitrogen also has led to an increase in the saturation magnetization. The room temperature magnetization increases from 119 emu/g for the host materials to 145 emu/g for the nitrides. The saturation magnetization at 4.2 K increases from 131 to 157 emu/g in the nitrides.

XRD on the aligned powder samples of the parent compound and the nitride are shown in Fig. 10(c) and (d), respectively. Indexing on the basis of the $Nd_3(Fe,Ti)_{29}$-type structure shows that in the parent compound, the (402) line is dominant. This suggests that the easy magnetization (EMD) of the parent compounds prefers to lie in the plane perpendicular to the (402) direction. By contrast, the nitrides showed a dominant (204) line, suggesting that the EMD of the nitrides is along the [001] direction.

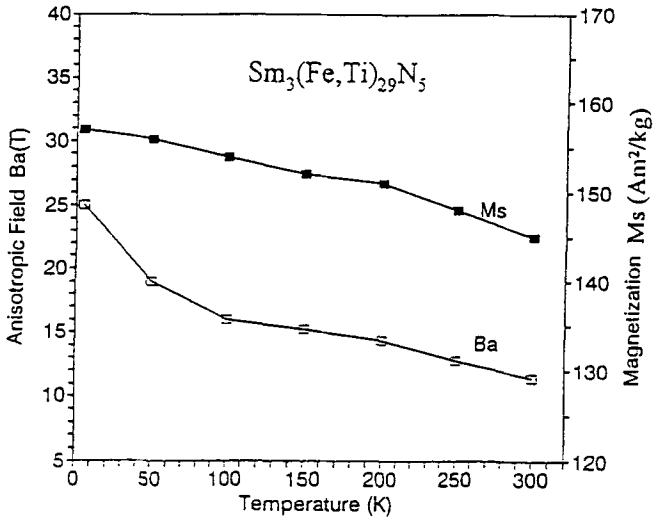

Fig. 13 Temperature dependence of anisotropy field and saturation magnetization in $Sm_3(Fe,Ti)_{29}N_5$ powders

Figure 13 shows the temperature dependence of the anisotropy field, B_a, and the saturation magnetization, M_{sat}, for the $Sm_3(Fe_{0.033}Ti_{0.067})_{29}N_9$ compounds. The anisotropy field, B_a, decreases monotonously with increasing temperature from 25 T at 4.2 K to 12 T at room temperature, and M_{sat} decreases from 154 to 145 emu/g.

To obtain more information regarding the magnetocrystalline anisotropy, a calculation of the anisotropy constants, K_i, was carried out. A procedure to derive the anisotropy constants from magnetization curves measured on magnetically aligned powders was developed by Huang et al. (Ref 14). The values of the anisotropy constants, K_i, can be derived by fitting the calculated magnetization curves to the experimental. A satisfactory fit (better than 2%) of the magnetization curves measured at 4.2 K was obtained using the parameters K_1 = 156 J/kg, K_2 = 208 J/kg, K_3 = 50 J/kg, for the nitride and K_1 = 895 J/kg, K_2 = –895 J/kg, and K_3 = 435 J/kg for its parent compound, as shown in Fig. 11 and 12. The value of K_3 for the nitride is very small compared to K_1 and K_2; this is in reasonable agreement with large uniaxial anisotropy field. In contrast to the nitride, the value of K_1 for the parent compound is positive, K_2 is large and negative, while K_3 is relatively large, suggesting that the anisotropy of the parent compound is nonuniaxial. The easy magnetization direction may be along the easy cone plane.

4. Conclusions

In summary, magnetically hard $Sm_2Fe_{17-x}Ga_xC_y$ (x = 2, 3 and y = 1, 1.5, 2, 2.5) ribbons were prepared with a high coercivity of 12.8 kOe at room temperature. The high coercivity obtained in this study may be attributed to the addition of Ga, which allows a higher solid solubility of carbon in the samples with a corresponding increase in the anisotropy field. Microstructure studies revealed the coexistence of an αFe and a 2:17-type phase. In samples annealed at high temperatures, the distribution of these phases is inhomogeneous with a coarse grain size leading to a shoulder in the demagnetization curve. However, in samples annealed at lower temperatures (700 °C), the grains are finer and uniform leading to a smooth demagnetization curve with a lower coercivity but with a higher reduced remanence, which are characteristic of nanocomposite exchange coupled magnets.

The R_2Fe_{17}-type $Sm_2Fe_{14-x}Co_xSi_2$ compounds with x = 0 to 7 crystallize in the Th_2Zn_{17}-type structure. Substitution of Co leads to an increase in Curie temperature from 514 K for x = 0 to 817 K for x = 7. It also enhances the uniaxial anisotropy, which changes from planar in $Sm_2Fe_{14-x}Co_xSi_2$ to uniaxial for $x \geq 4$. The $Sm_2Fe_{14-x}Co_xSi_2N_y$ nitrides maintain the Th_2Zn_{17} type structure but with a unit-cell expansion $\Delta V/V$ up to 5% compared to the host materials. The $Sm_2Fe_{14-x}Co_xSi_2C_z$ carbides with z = 1 maintain the Th_2Zn_{17}-type structure and transform to the $BaCd_{11}$-type structure for z = 2. The room temperature anisotropy field obtained is 100 kOe for $Sm_2Fe_{14}Si_2C$ and 175 kOe for $Sm_2Fe_{10}Co_4Si_2N_{2.3}$. A very large anisotropy field is also observed at low temperature (1.5 K) with a value of 204 kOe for $Sm_2Fe_{14}Si_2C$ and 276 kOe for $Sm_2Fe_{10}Co_4Si_2N_{2.3}$.

$Sm_3(Fe_{0.933}Ti_{0.067})_{29}N_5$ and the parent compounds crystallize in the $Nd_3(Fe,Ti)_{29}$-type structure. These compounds exhibit a ferromagnetic coupling with a Curie temperature of 750 K and a saturation magnetization of 157 emu/g at 4.2 K. $Sm_3(Fe_{0.933}Ti_{0.067})_{29}$ compounds exhibit uniaxial anisotropy from 4.2 K to the ordering temperature. The anisotropy field is 12 T at room temperature and 25 T at 4.2 K. The nitrides and carbides studied here all have excellent intrinsic magnetic properties and can be new candidates for permanent magnet developments.

Acknowledgment

This work was supported by U.S. Army Research Office #DAAL03-92-G-0086.

References

1. J.M.D. Coey and H. Sun, *J. Magn. Magn. Mater.*, Vol 87, 1990, p L251
2. H. Sun, J.M.D. Coey, Y. Otani, and D.P.F. Herly, *J. Phys., Condens. Matter*, Vol 2, 1990, p 6465
3. R.B. Helmholdt and K.H.J. Bushow, *J. Less-Common Met.*, Vol 144, 1988, p L33
4. T.H. Jacobs, M.W. Dirken, R.C. Thiel, L.J. De Jonph, and K.H.J. Buschow, *J. Magn. Mater.*, Vol 83, 1990, p 293
5. B.G. Shen, F.W. Wang, L.S. Kong, L. Cao, and W.S. Zhan, *J. Appl. Phys., 75*, 1994, p 6253
6. B.G. Shen, L.S. Kong, F.W. Wang, and L. Cao, *Appl. Phys. Lett.*, Vol 63, 1993, p 2288
7. Y.H. Zheng, A.S. Murthy, and G.C. Hadjipanayis (manuscript in preparation)
8. F. Pourarian, R. Obermyer, Y. Zheng, S. Sankar, and W.E. Wallance, *J. Appl. Phys.*, Vol 73, 1993, p 6272
9. C.M. Gubbens and K.H.J. Buschow, *Phys. Status Solidi (A)*, Vol 34, 1976, p 729
10. F. Pouarian, R. Obermyer, Y. Zhang, S.G. Sankar, and W.E. Wallace, *MMM93 Abstract*, 1993, p 239

11. S.J. Collocot, R.K. Day, J.B. Dunlop, and R.I. Lewis, *Proc. 7th Int. Symp. on Magnetic Anisotropy and Coercivity in R-T Alloys* (Canberra), July 1992, p 437

12. F.M. Yang, B. Nansunjilegal, H.Y. Pan, J. Wang, R. Zhao, B.P. Hu, Y.Z. Wang, H.S. Li, and J.M. Cadogan, to be submitted to *J. Magn. Magn. Mater.*

13. E.W. Singleton and G.C. Hadjipanayis, *J. Appl. Phys.*, Vol 75 (No. 10), 15 May 1994f

14. Y.K. Huang, C.H. Wu, Y.C. Chuang, F.M. Yang, and F.D. deBoer, *J. Less-Common Met.*, Vol 132, 1987, p 313